Bacterial Growth and Adaptation in Microdroplet Chemostats**

*Slawomir Jakiela, Tomasz S. Kaminski, Olgierd Cybulski, Douglas B. Weibel, and Piotr Garstecki**

We describe herein microfluidic technology for manipulating and monitoring continuous growth of populations of bacteria. A system consisting of approximately ten input and output channels controls more than 100 microdroplet chemostats and enables the manipulation of chemical factors in each micro-chemostat independently over time. Herein, we characterize the dynamics of bacterial populations in microdroplet chemostats and cellular responses to a range of stable or changing antibiotic concentrations. This method allows for parallel, long-term studies of microbial ecology, physiology, evolution, and adaptation to chemical environments.

The introduction of the chemostat by Leo Szilard[1] was a milestone in the field of microbiology. Chemostats facilitate the continuous culture of bacteria, yeast, and algae by continuously replenishing a constant volume of fluid to maintain specific concentrations of cells and growth factors.[1,2] Chemostats have facilitated a wide-range of studies, including microbial ecology,[3] predator–prey dynamics,[4] and the evolution of drug resistance.[5,6] The consumption of large quantities of reagents and the significant operational challenges of traditional chemostats limit their use.

Single-phase, microfluidic versions of chemostats minimize incubation volumes,[7–10] and yet are limited by their complexity: the proportionality between the number of input/ output controls and the number of chemostats hamper large scale parallelization. Single-phase microfluidic systems are prone to biofilm formation, which makes them either single-use devices[9] or requiring additional steps to minimize cell adhesion.[8] Droplet microfluidics[11] offer a unique solution to creating many parallel chemostats. The earliest example of this technology in microbiology was first demonstrated by Joshua Lederberg nearly 60 years ago.[12] In the interim, the field of microfluidics solved many of the technical challenges associated with using this approach to study microbes. Compartmentalizing cells and nutrients in microdroplets of liquid can reduce the complexity and cost of operating many parallel chemostats. Recently, bacteria have been incubated in droplets in channels over short time intervals,[13–17] however sustained cell growth over hundreds of generations in a series of fully addressable microdroplets has not been possible.

Herein, we describe an automated microdroplet system that transcends existing challenges and enables users to manipulate the chemical composition of droplets for long-term bacterial studies. The microfluidic system (Figure 1) performs three functions: 1) formation of microdroplets containing cells, reagents, and soluble growth factors; 2) cycling microdroplets for cell incubation and monitoring; and 3) splitting and fusing microdroplets to control the concentration of chemical factors over time.

After loading the reservoirs with liquid samples, we used a source of pressure and external valves to regulate the flow of

[*] Dr. S. Jakiela,[+] T. S. Kaminski,[+] Dr. O. Cybulski, Prof. P. Garstecki
Institute of Physical Chemistry, Polish Academy of Sciences
Kasprzaka 44/52, 01-224 Warsaw (Poland)
E-mail: garst@ichf.edu.pl
Homepage: http://pepe.ichf.edu.pl/pgarstecki/index.html

Prof. D. B. Weibel
Department of Biochemistry, University of Wisconsin-Madison
433 Babcock Drive, Madison, WI 53706 (USA)

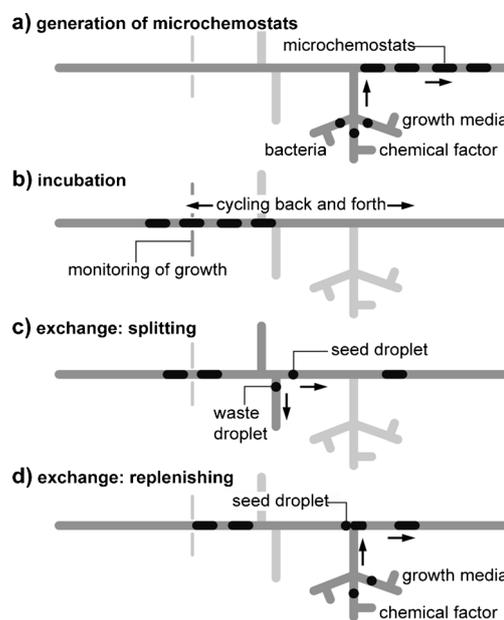[+] These authors contributed equally to this work.

Figure 1. Diagram of the operation of the microdroplet chemostat system. a) Fusing droplets of bacteria, growth media, and chemical factors creates a sequence of microdroplets containing encapsulated bacteria. b) Microdroplets are cycled in the incubation segment and cell growth is monitored. c) Each microdroplet is split into a seed droplet and a waste droplet. d) The seed droplet is fused to a micro-droplet containing nutrient media and chemical factors.

oil (the carrier fluid), aqueous growth media, and a suspension of bacterial cells. We generated a sequence of microdroplets seeded with cells, nutrients, and reagents by coalescing smaller droplets of different solutions.[15] Real-time video feedback enabled us to administer volumes with an accuracy of around 0.3%.

We created a sequence of 164 microdroplet chemostats and cycled them back and forth in pressure-driven flow-controlled channels with two pairs of (in/out) valves at each end of the channel (Figure 2). The microchemostats periodically passed through an in situ, waveguide spectrophotometer that measured the absorbance of light ($\lambda = 600$ nm) passing through each droplet over a five millimeter optical path.

At user-defined intervals, the system exchanges a fraction of the volume of each microdroplet chemostat. First, a microdroplet was accurately divided into two preprogrammed volumes: a waste and a seed droplet (Supporting Information, Video S1, Figures S3,S4). The waste droplet was removed from the system and the seed droplet was fused (Video S2) with a microdroplet containing fresh reagents. Using this approach, we controlled the concentration of cells and
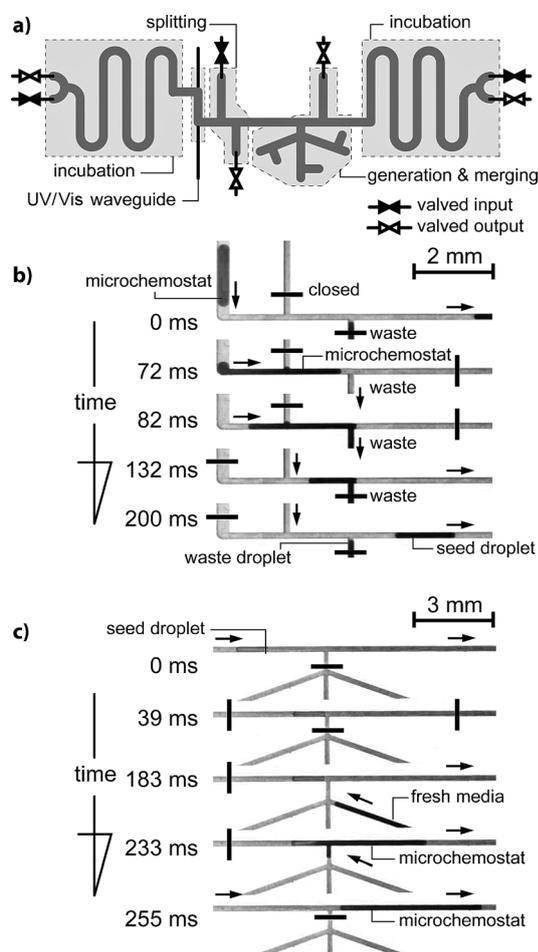
reagents in microdroplets over 10–100 hours (Video S3) and controlled the concentration of soluble factors with an accuracy of approximately 0.8% (Figure S3,S4). The transfer of a fraction of the growing bacterial population—with its characteristic genotype and phenotype—to new microdroplets containing fresh media and user-defined chemical compositions enabled us to perform experiments of long-term cell growth.

To check the dynamics of growth in microdroplet chemostats we prepared microdroplets (volume: 1.28 μL) containing a suspension of *Escherichia coli* cells (strain ATCC 25992) at a density of $(1.09 \pm 0.13 \times 10^7 \text{ cfu mL}^{-1})$ in LBK media buffered with pH 7.0 PIPES, which gives the maximal growth rate under anaerobic conditions.[18] A single droplet contained approximately 14 000 cells (OD = 0.025) at the beginning of cultivation. We cycled the droplets for 600 minutes and continuously monitored cell density. Growth in microdroplet chemostats (Figure 3 a) was similar to growth in bulk liquid culture, including the initial exponential-growth phase, log-phase growth, and the stage of saturation. The number of cells $N(t)$ in microdroplet chemostats followed Monod's model:[19] $N(t) = N_0 e^{\mu(C(t))t}$, where N_0 is the initial number of cells, $\mu(C(t)) = (\mu_{max}(C(t))/(K_M + C(t)))$ is the specific growth rate of bacteria (one hour), $C(t)$ is the concentration of the rate limiting nutrient (g mL^{-1}), μ_{max} is the maximum growth rate (1 h), and K_M (g mL^{-1}) is the saturation parameter corresponding to the substrate concentration that yields half the maximum growth rate. The values of the constants that we determined from fitting the model are consistent with values for *E. coli* growing in rich nutrient broth.

The conditions the in microdroplet chemostats can be controlled using three parameters: 1) the chemical composition of the growth media; 2) the frequency of exchanging the
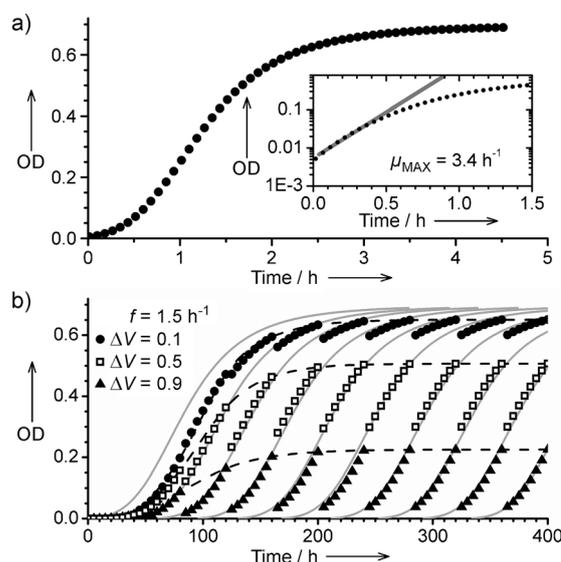

Figure 2. a) Diagram of the layout of the microfluidic device. b) A sequence of micrographs illustrating the splitting of one microdroplet into a seed droplet and waste droplets with pre-programmed volumes. c) A sequence of micrographs illustrating the fusion of the seed droplet with fresh media to control the chemical composition and number of cells in a microchemostat.

Figure 3. a) Representative growth curve of *E coli* ATCC 25992 cells in a microdroplet chemostat. Inset: a calculation of the growth rate by fitting the exponential function. b) Three repetitive growth curves acquired for an extended period of time and with different fractions of exchanged media (either 0.1, 0.5, or 0.9 of the droplet volume). Experimental data points are in good agreement with theoretical curves depicting Monod's model (gray lines).

culture media; and 3) the fraction of the microdroplet volume that is exchanged. To probe the role of parameters (2) and (3) we created a sequence of 1.28 μL droplets with a low cell concentration $(1.09 \pm 0.13 \times 10^7 \, \mathrm{cfu\,mL^{-1}})$ and iterated the steps of cycling and exchanging media. The concentration of cells followed Monod's model (Figure 3a). Initially, the concentration of cells increased with every iteration and reached a periodic trajectory after several iterations (Figure 3b). The shapes of the growth curves illustrate the approach to a stable cell density N_{SAT} at the moment of exchanging liquids. The region of Monod's curve probed in each (ith) microchemostat and N_{SAT} depends on the interval T_i between——or frequency $f_i = T_i^{-1}$ of——exchanges, and the fraction ΔV_i of the volume V of the droplet that is exchanged.

Cell density in a traditional chemostat depends on the dilution ratio $D = Q/V$, where Q is the flow rate. The analogous parameter in microdroplet chemostats is $D = f \Delta V/V$. To test how N_{SAT} depends on D we created a sequence of 54 microdroplets, starting with, $N_0 = 1.09 \pm 0.13 \times 10^7 \, \mathrm{cfu\,mL^{-1}}$ and tested a 9×6 matrix of values of D where $\Delta V/V \in (0.1, 0.9)$ with a step of 0.1 and $f \in (0.5, 3)$ [1 h] with a step of 0.5 [1 h]. At low values of f and $\Delta V/V$, cell density is high. Increasing D decreases N_{SAT}; at extreme values of f and $\Delta V/V$, the culture is unable to regrow within the interval T. Figure S7 shows that the density of bacterial communities in microdroplet chemostats follows a similar trend to those in traditional chemostats. An appropriate choice of f and $\Delta V/V$ enabled us to reduce the changes in the optical density that occur during the exchange of media to less than 10%, providing a close approximation of continuous exchange of media in a classical chemostat (Figure S8).

Using numerical simulations of Monod's model we confirmed that the dynamic stability of the bacterial populations (i.e. of N_{SAT}) agreed with the small error ($\sigma_V < 1\%$) in exchanging the volume ΔV of the microchemostat (Figure S9). The precision of liquid handling gave exceptionally small variability in the density of bacterial populations: a control experiment conducted over 50 hours yielded variability in N_{SAT} of less than or equal to 5% (Figure S9).

Parallel experiments of microbial population dynamics—including studies of predator/prey and syntrophic interactions—and the response and adaptation of bacteria to chemical and environmental stresses require that no cross-contamination occurs between the microchemostats. Long-term control experiments monitoring the concentration of fluorescein in circulating droplets (Figure S2) and with bacteria, in which we compared the growth rate and saturation density of cells in adjacent microdroplets that either contained LBK nutrient media or LBK admixed with chloramphenicol $(10 \, \mathrm{\mu g\,mL^{-1}})$, suggested no cross-contamination (Figure S10). Low levels of cross-contamination would be expected,[20] however the physical dimensions of the microdroplets and the large separation between them in our system reduces the mass exchange between droplets to negligible levels. Other factors that can reduce cross-contamination include the use of small concentrations of surfactant or fluorinated oils in the continuous phase.

As an application of this system, we determined the parameters of the growth curves of $E. coli$ as a function of the concentration of tetracycline. Parameters extracted from fits of Monod's equation quantitatively determine the effect of the antibiotic on the growth rate (Figure S11). Importantly, this system allowed us to study the response and adaptation of microorganisms to changing chemical environments. We studied the response of $E. coli$ cells to changes in the concentration of chloramphenicol (C_{CHL}). We grew cells in microdroplet chemostats to a steady state in the absence of stress for four hours ($f = 3 \, \mathrm{h^{-1}}$, $\Delta V = 0.5$), then applied one of three different values of C_{CHL} and monitored the dynamics of bacterial populations over 45 hours (Figure 4b–d). The growth rate of the bacteria decreased as chloramphenicol was added and continued to decrease for several generations of growth in the microdroplet chemostats. After a period of time, which depended on C_{CHL}, the bacteria adapted, growth accelerated, and returned to the initial rate. There are several possible explanations for the observed increase in growth rate, including changes in membrane properties,[6] drug efflux, or changes in the structure of the ribosome,[21] which is targeted by chloramphenicol.

We next studied the response of populations of $E. coli$ to slowly increasing C_{CHL} (Figure S12). We prepared 15 microchemostats consisting of three groups of five microdroplets that were treated with increasing C_{CHL} at rates of 0.006, 0.01, or 0.015 $\mathrm{\mu g\,mL^{-1}\,h^{-1}}$. The maximum standard deviation in the absorbance between microdroplets in each group was 5.7% (for a rate of 0.006 $\mathrm{\mu g\,mL^{-1}\,h^{-1}}$), 6.1% (0.01), and 7.1%

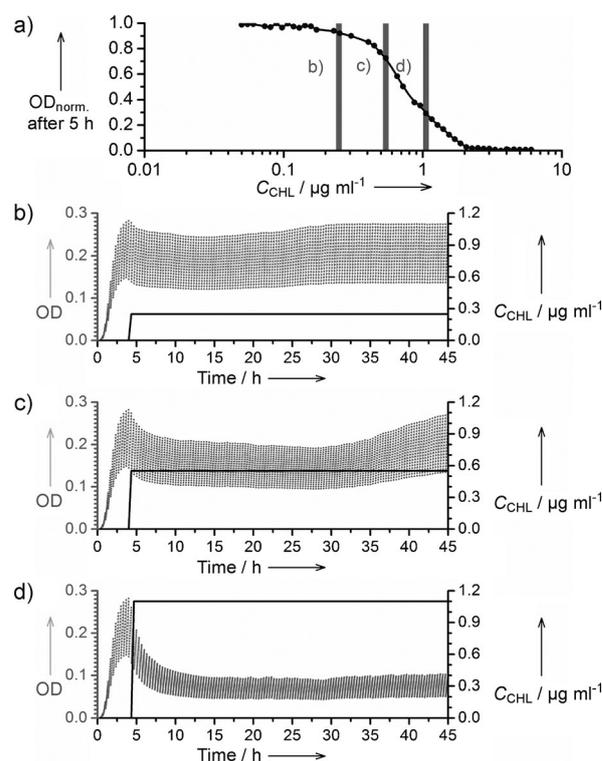***Figure 4.*** a) A plot of the relationship between the normalized optical absorbance of E. coli cells ($\lambda = 600$ nm) and C_{CHL}. Vertical bars indicate concentrations used in the adaptation experiments (b–d). The right axes of plots (b–d) show the concentration of antibiotic (C_{CHL}, black line), and the left axes show the optical density measured in the microchemostats (gray dots).

(0.015) throughout the 45-hour experiment. Higher rates of chloramphenicol addition produced more variability in growth rates. This observation prompts questions about the relation between the diversity of mutations arising in the population and the level of stress to which it is subjected. Another possible explanation is the growth of the persisting cells that survive antibiotic dosing.[7] We are currently studying the influence of the rate of antibiotic addition on genetic variation, which is beyond the scope of this paper.

In summary, microdroplet chemostats enable long-term, highly parallel studies of cell growth in response to extracellular chemical stress. To the best of our knowledge, this is the first demonstration of a fully automated droplet microfluidic device that offers scalability in the number of parallel microchemostats. Only the physical dimensions and the frequency of droplet formation and manipulation limit the scalability of the system.

Previous studies have demonstrated the cultivation of microorganisms inside droplets, which can be advantageous because of several characteristics, including: 1) massive parallelization;[22–24] 2) stochastic confinement;[16] and 3) automation.[14,15] The longest cultivation times reported to-date have been several bacterial generations owing to limited nutrient availability and the accumulation of secondary metabolites. The microchemostat system we report enables the long-term cultivation of bacteria by exchanging small volumes of liquids between microdroplets and parallel studies of the effect of fluctuating chemical environments on the adaptation and dynamics of microbial populations. A remaining technical challenge is to construct the system in a stiff, yet gas-permeable polymer that supports aerobic metabolism and alleviates the requirement for buffering the growth media. The system can be readily expanded for an additional feedback control loop to adjust the parameters for media and reagent exchange (f, $\Delta V/V$) in response to measured rates of growth. This capability will make it possible to perform long-term experiments on the trajectories of adaptation of microbial communities to chemical stresses. Chemostat studies have demonstrated the remarkably rapid adaptation of bacteria to environmental changes.[6] Our approach complements these experiments by introducing a method for the parallel study of hundreds of individual microchemostats. Importantly, the operational complexity of the system is low and users can rapidly adjust the phase of bacterial growth in experiments and the size and density of the bacterial populations.

Importantly, our system can be integrated with the capability for splitting large (ca. microliter) droplets containing populations of microorganisms into thousands of monodisperse small (picoliter) droplets[25] for further screening at the single cell level.[22–24] This could open new areas of study, including the distribution of fitness or gene expression in a population subject to changes in the chemical environment in which it grows. These capabilities provide new opportunities for studying the genetic and phenotypic adaptation of

bacteria and open a new window for studies of microbial evolution.

[1] A. Novick, L. Szilard, *Science* **1950**, *112*, 715–716.
[2] T. James, *Annu. Rev. Microbiol.* **1961**, *15*, 27–46.
[3] H. Topiwala, G. Hamer, *Biotechnol. Bioeng.* **1971**, *13*, 919–922.
[4] L. Becks, F. M. Hilker, H. Malchow, K. Jurgens, H. Arndt, *Nature* **2005**, *435*, 1226–1229.
[5] H. H. Lee, M. N. Molla, C. R. Cantor, J. J. Collins, *Nature* **2010**, *467*, 82–85.
[6] E. Toprak, A. Veres, J.-B. Michel, R. Chait, D. L. Hartl, R. Kishony, *Nat. Genet.* **2012**, *44*, 101–105.
[7] N. Q. Balaban, J. Merrin, R. Chait, L. Kowalik, S. Leibler, *Science* **2004**, *305*, 1622–1625.
[8] F. K. Balagadde, L. C. You, C. L. Hansen, F. H. Arnold, S. R. Quake, *Science* **2005**, *309*, 137–140.
[9] A. Groisman, C. Lobo, H. J. Cho, J. K. Campbell, Y. S. Dufour, A. M. Stevens, A. Levchenko, *Nat. Methods* **2005**, *2*, 685–689.
[10] S. H. Au, S. C. C. Shih, A. R. Wheeler, *Biomed. Microdevices* **2011**, *13*, 41–50.
[11] A. B. Theberge, F. Courtois, Y. Schaerli, M. Fischlechner, C. Abell, F. Hollfelder, W. T. S. Huck, *Angew. Chem.* **2010**, *122*, 5982–6005; *Angew. Chem. Int. Ed.* **2010**, *49*, 5846–5868.
[12] J. Ledeberg, *J. Bacteriol.* **1954**, *68*, 258–259.
[13] K. Leung, H. Zahn, T. Leaver, K. M. Konwar, N. W. Hanson, A. P. Page, C.-C. Lo, P. S. Chain, S. J. Hallam, C. L. Hansen, *Proc. Natl. Acad. Sci. USA* **2012**, *109*, 7665–7670.
[14] L. Baraban, F. Bertholle, M. L. M. Salverda, N. Bremond, P. Panizza, J. Baudry, J. A. G. M. de Visser, J. Bibette, *Lab Chip* **2011**, *11*, 4057–4062.
[15] K. Churski, T. S. Kaminski, S. Jakiela, W. Kamysz, W. Baranska-Rybak, D. B. Weibel, P. Garstecki, *Lab Chip* **2012**, *12*, 1629–1637.
[16] J. Q. Boedicker, M. E. Vincent, R. F. Ismagilov, *Angew. Chem.* **2009**, *121*, 6022–6025; *Angew. Chem. Int. Ed.* **2009**, *48*, 5908–5911.
[17] R. Derda, S. K. Y. Tang, G. M. Whitesides, *Angew. Chem.* **2010**, *122*, 5429–5432; *Angew. Chem. Int. Ed.* **2010**, *49*, 5301–5304.
[18] D. Blankenhorn, J. Phillips, J. L. Slonczewski, *J. Bacteriol.* **1999**, *181*, 2209–2216.
[19] J. Monod, *Ann. Inst. Pasteur* **1950**, *79*, 390–410.
[20] Y. Skhiri, et al., *Soft Matter* **2012**, *8*, 10618–10627.
[21] O. Pongs, R. Bald, V. Erdmann, *Proc. Natl. Acad. Sci. USA* **1973**, *70*, 2229–2233.
[22] E. Brouzes, M. Medkova, N. Savenelli, D. Marran, M. Twardowski, J. B. Hutchison, J. M. Rothberg, D. R. Link, N. Perrimon, M. L. Samuels, *Proc. Natl. Acad. Sci. USA* **2009**, *106*, 14195–14200.
[23] J. J. Agresti, E. Antipov, A. R. Abate, K. Ahn, A. C. Rowat, J.-C. Baret, M. Marquez, A. M. Klibanov, A. D. Griffiths, D. A. Weitz, *Proc. Natl. Acad. Sci. USA* **2010**, *107*, 4004–4009.
[24] J.-C. Baret, Y. Beck, I. Billas-Massobrio, D. Moras, A. D. Griffiths, *Chem. Biol.* **2010**, *17*, 528–536.
[25] T. S. Kaminski, S. Jakiela, M. A. Czekalska, W. Postek, P. Garstecki, *Lab Chip* **2012**, *12*, 3995–4002.